James Webb Space Telescope (JWST)

Mid-Infrared Instrument (MIRI)

MIRI FM Performance Test Report

A Further Analysis of JPL MIRI NRB High SNR Data

Author: Patrice Bouchet & René Gastaud CEA/SAp Date: 30/07/2012

Approved: Date:

(possibly your national project manager or co-PI)

Reviewed: Date:

(MIRI EC Instrument Scientist (Alistair))

DOCUMENT CHANGE DETAILS

Issue	Date	Page	Description Of Change	Comment
A	30/07/2012	All	First Draft Issue.	
1	01/08/2012	1, 8, 9, 10	Abstract and conclusion modified; discrepancy with TG cleared out.	

PAGE INTENTIONALLY LEFT BLANK

TABLE OF CONTENTS

LIST OF TABLES

LIST OF FIGURES

1 ABSTRACT

The goal of this work was primarily to check our analysis tools by comparing our results with those from Tom Green's analysis (JPL_MIRI_high_SNR_data_analysis_2012May11.pdf). Surprisingly our results are significantly different from those referred to. The origin of the discrepancy lies in the data subset used in both analysis. For the present work we set ourselves in the best possible case.

2 PROCEDURE

We use the same data as Tom:

MIRI_7157_27_S_20120417-201316_SCE3.fits and MIRI_7157_28_S_20120417-203313_SCE3.fits

There are no corrupted frames. The length of a ramp, ngroup = 50, and there are 8 ramps in both observations.

To reduce the data MIRI_7157_27_S_20120417-201316_SCE3, we drop the first two ramps, and in each ramp we discard the 4 first frames and the last one.

To reduce the data MIRI_7157_28_S_20120417-203313_SCE3, we drop the first ramp, and the 4 first frames and the last one.

This was done after checking that, for one illuminated point, (Xc, Yc) = (805, 794), a line fits with small deviations the data points (figure 1).

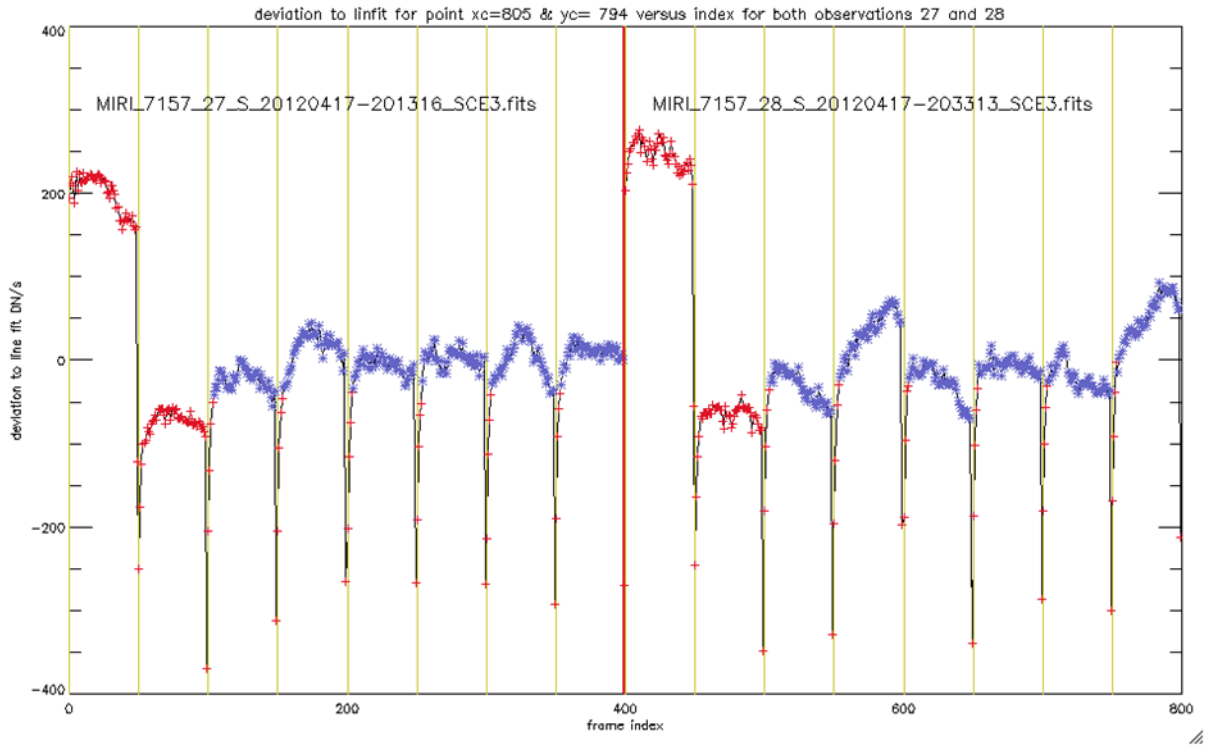

Figure 1: Residuals (true signal – fit) for each ramp for both exposures; fits have been computed independently for each exposures. The red points are the ones excluded for our analysis.

We then perform aperture photometry with the "aper" command, which is the IRAF equivalent of DAOPHOT in the IRAF environment. We use an aperture of 150 pixels radius, and an inner sky annulus between pixels 180 and 210 (figure 2). It appeared that using the same aperture as Tom (73 pixels radius) was not large enough to include the entire signal from the point-like source as can be seen in figure 3. Note that figure 3 refers to the data MIRI_7157_27, and that the same plot using the data MIRI_7157_28 superimposes exactly on it.

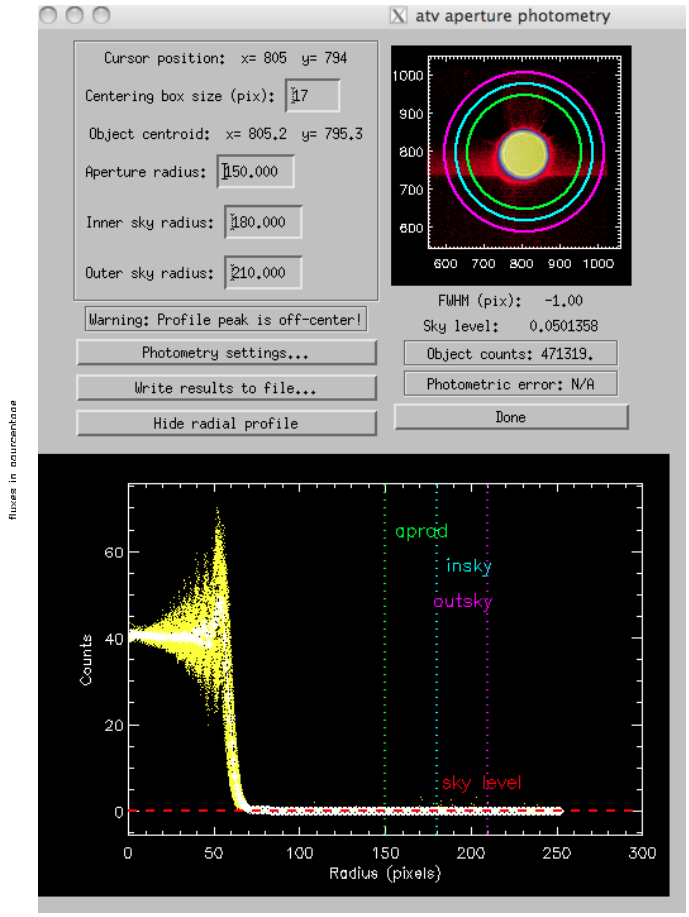

Figure 2: Radial profile and apertures of illuminated region of the aperture near (805, 794). Y-axis units are DN/s and X units are in pixels.

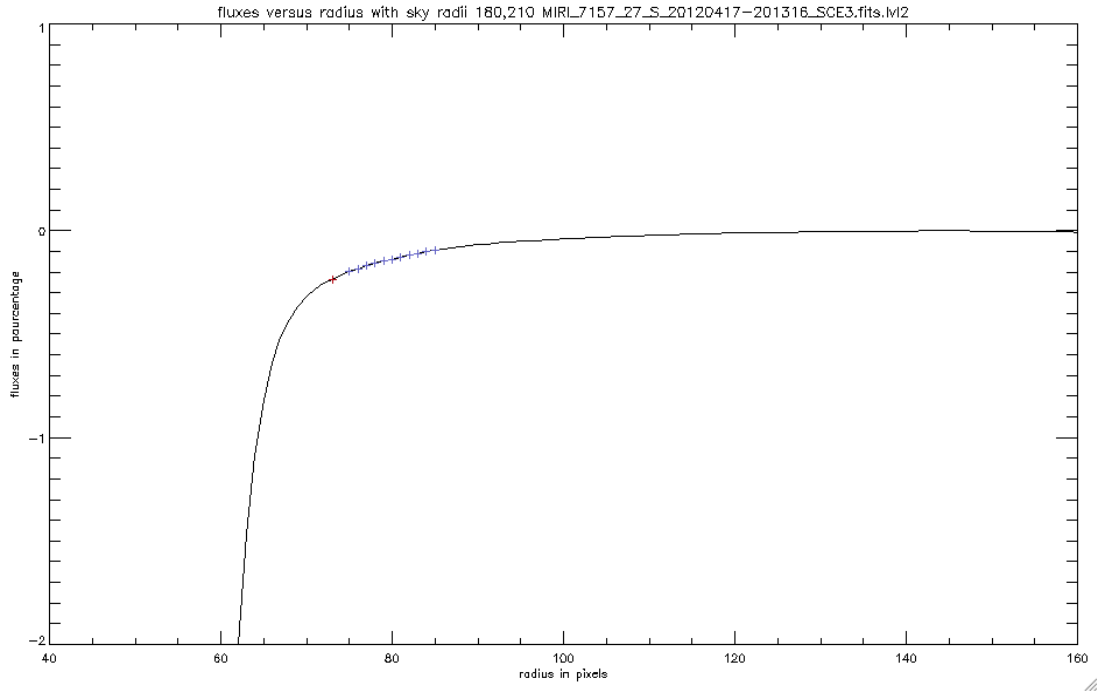

Figure 3: Profile along the line passing through the center of the source. Blue points indicate the sky annulus region used by Tom.

Results from our aperture photometry are given in Table 1.

Exposure	Integration	Flux (DN/s)	Electrons
MIRI_7157_27	1	463235.	3.54780e+08
	2	469315.	3.59437e+08
	3	470151.	3.60077e+08
	4	470886.	3.60640e+08
	5	471067.	3.60778e+08
	6	470929.	3.60673e+08
	7	471278.	3.60940e+08
	8	471170.	3.60857e+08
MIRI_7157_28	1	468458.	3.58780e+08
	2	471568.	3.61162e+08
	3	471222.	3.60897e+08
	4	471282.	3.60943e+08
	5	471233.	3.60906e+08
	6	471214.	3.60891e+08
	7	471366.	3.61007e+08
	8	471159.	3.60849e+08

Table 1 : Aperture (805, 794) photometry results; conversion of flux to electrons is made with E = F x Gain x Tint, with Gain = 5.5 and Tint = 139.250 s.

It can be seen from Table 1 that although "our" fluxes are systematically slightly higher than the ones given in Tom's Table 1 (due to the larger aperture used to include the entire signal), both set compare well.

We apply the same method as the one described in **MIRI-TR-00003-CEA** for measuring the signal-to-noise ratio and the noise, which we compare with the theoretical noise. We use as input a cube of slopes (DN/s) one per ramp, so we have 7 images (first image is discarded).

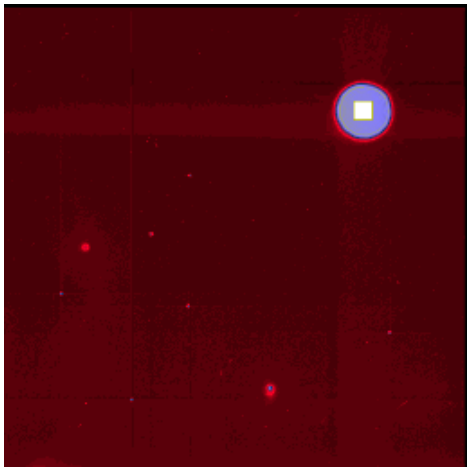

We then consider a squared area (41 x 41 pixels) centered on the illuminated disk (see figure 4).
We assume that the illumination level is constant inside this square area at a mean value computed for various cases (Tables 2 & 3), and we compute the shot noise for a gain of 5.5 and a read noise of 5 e^- (note that accordingly to the formula used for computing the theoretical noise this parameter could be neglected).
See Table 2 & 3 for the results.

Figure 4 : the squared area centered on the illuminated disk used for our analysis.

The theoretical noise is computed from the formula used by Mike Ressler's "Interim SNR Analysis" (MIRI DFM 426):

$$\sigma_m^2 = \frac{1}{N^2-1}\left(\frac{12N\,\sigma_{read}^2}{T_{int}^2} + \frac{6}{5}\cdot\frac{F(N^2+1)}{T_{int}}\right)$$

	Mean Flux		σ Measured		σ Theoretical		SNR Measured		SNR Theoretic	
	Odd	Even	Odd	Even	Odd	Even	Odd	Even	Odd	Even
Drift	40.120	40.590	0.268	0.269	0.250	0.252	150	151	160	161
No Drift	40.120	40.590	0.365	0.330	0.250	0.252	110	122	160	161

Table 2 : Results for MIRI_7157_27 for odd and even columns; these values are given per pixel

	Mean Flux		σ Measured		σ Theoretical		SNR Measured		SNR Theoretic	
	Odd	Even	Odd	Even	Odd	Even	Odd	Even	Odd	Even
Drift	40.123	40.590	0.268	0.269	0.253	0.254	150	151	157	160
No Drift	40.123	40.590	0.365	0.330	0.253	0.254	110	123	157	160

Table 3: : Same as Table 2 for exposure MIRI_7157_28

	MIRI_7157_27: SNR Meas. / SNR Theor.		MIRI_7157_28: SNR Meas. / SNR Theor.	
	Odd	Even	Odd	Even
Drift Corrected	0.938	0.938	0.955	0.944
No Drift Correction	0.688	0.758	0.700	0.769

Table 4: The ratios of the measured Signal-to-Noise over the theoretical ones with and without drift correction, and for odd and even columns.

Tables 4 shows that after drift correction our measured noise is close to the theoretical at about the 5% level. Note that the drift correction does not multiply the SNR by 3 as in previous analysis of other set of data but only by ~ 1.4 because the fluctuations of each pixel are not correlated.

4 2ND METHOD

We now analyse the data in the same way as Tom. Data are given in Table 1, and Figure 5 displays the photometric fluxes of the source versus time. It can be seen that exposure 27 is not "stabilized", and we therefore consider in what follows only exposure 28. From the fluxes vector we compute the mean, the standard deviation and the ratio of them which we consider to be a good representative of the Signal-to-Noise ratio (SNR) which we show in Table 5.

Mean Flux (DN/s)		Mean Flux (Electrons)		SNR	Case
Mean	σ	Mean	σ		
470938	1009.98	3.60679e+08	773516.	466	0
471292	138.772	3.60951e+08	105512.	3421	1
471246	70.8700	3.60915e+08	54281.6	6649	2

Table 5: Mean fluxes, standard deviations and Signal-to-Noise for the data corresponding to the exposure MIRI_7157_28 in three cases; 0 = all the data points are considered; 1 = the first data point is discarded; 2 = the first two points are discarded.

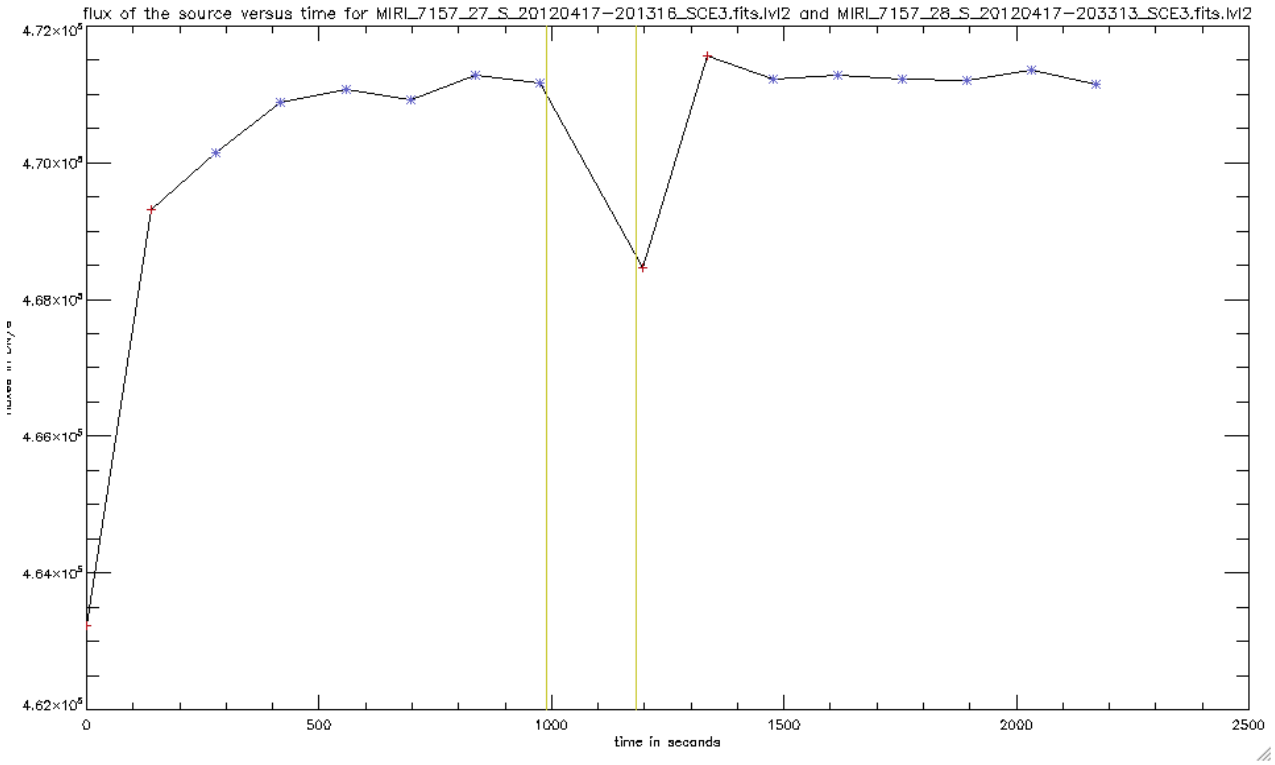

Figure 5 : Level 2 data for MIRI_7157_27 and MIRI_7157_28 versus time; red points correspond to the frames that have been discarded; the two horizontal lines distinguish between both exposures. Y-axis units are DN/s and X-axis units are seconds.

Clearly, only case 2 is pertinent. The standard deviation is thus $\sigma = 54282.$ Tom finds $\sigma = 1.496\ \mathrm{E6}$ **because he considers both exposures 27 and 28.** We note that our worst case gives $\sigma = 0.773\ \mathrm{E6}$ (all the data points of exposure 28).

For a flux = 4.71246E5 DN/s, the theoretical noise computed as above is 27 DN/s, which yields to a theoretical Signal-to-Noise ratio $SNR_{Theo.}$ = 17336. Our best $SNR_{Meas.}$ (6649) is thus **0.38 x SNR_{Theo}**.

This value is very far from Tom's $SNR_{Meas.}$ = 223 which is indeed only 1.28% of the theoretical Signal-to-Noise ratio. Again, Tom uses the worst case while we use the more favourable one.

5 ANALYSIS OF A SMALLER APERTURE

We analyse now the point like source located at (599, 176), whose peak signal is 46.84 DN/s. Aperture photometry is performed with a radius of 20 pixels, the sky region being defined by the annulus comprised between the circles of radius 30 and 40 pixels (see Figure 6). These values are chosen accordingly to the image profile shown in Figure 7.

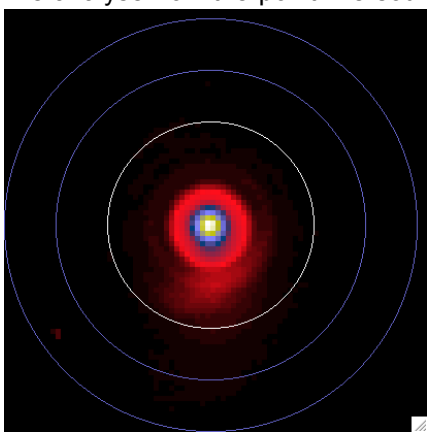

We obtain the flux intensity of the source for the 8 slopes of exposure MIRI_7157_28 (Table 6)

Figure 6 : 41 x 41 pixels image of the point like source located (599, 176); the aperture used for performing the photometry is 20 pixel radius (white circle), and the sky ring annulus is defined by the circles (in blue) of radius 30 and 40 pixels.

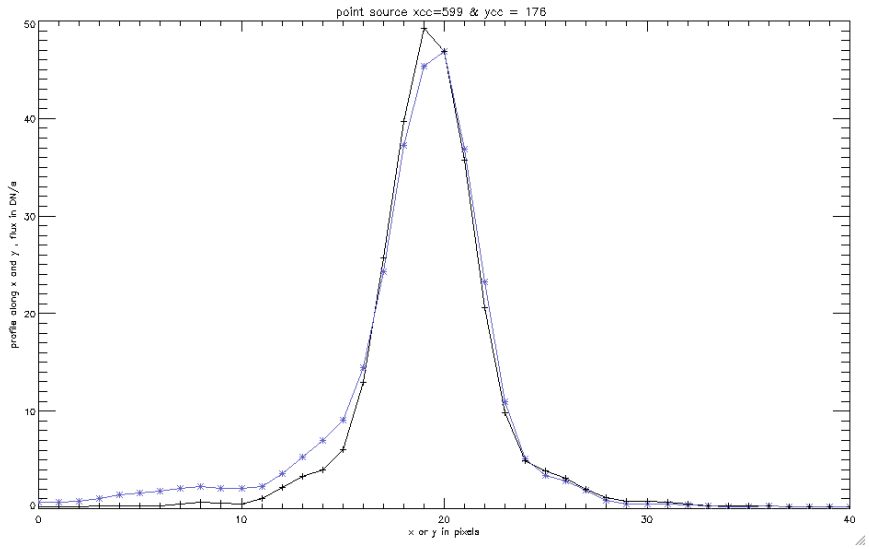

Figure 7 : The (599, 176) source profile; the entire signal of the source is comprised in a disk of 20 pixels radius.

n	Flux (DN/s)	Flux (Electrons)
1	2201.79	1.68630e+06
2	2208.01	1.69106e+06
3	2197.23	1.68280e+06
4	2203.00	1.68722e+06
5	2205.28	1.68897e+06
6	2207.81	1.69091e+06
7	2205.50	1.68914e+06
8	2204.28	1.68820e+06

Table 6: Aperture photometry of (599, 176) for the 8 slopes of the exposure MIRI_7157_28; note that Fux(Electrons) = Flux(DN/s) x Gain x tint, with Gain = 5.5 e^- /DN, tint = 139.25 s.

Our aperture photometry yields to: mean flux intensity of F = 2203 DN/s, σ = 3.61 DN/s, and SNR = 628.

The theoretical noise computed as above (with a gain = 5.5) is: 1.86 DN/s. That is about a factor 2 between the measured and the theoretical noise.

The flux in electrons is: 1.69 E6, which yields to $SNR_{Theoretical}$ ~ sqrt(1.69 E6) ~ 1300 and

$$SNR_{Measured} / SNR_{Theoretical} = 0.48$$

6 CONCLUSION

We have measured signal-to-noise ratios 38% to 48% (for bright to moderately illuminated sources respectively) lower than the computed theoretical ones. Our results are significantly different from Tom Green's. However, it has to be noted that Tom considers the worst case while we made a significant "cleaning" of the data, resulting in the use of half of them. We show also that applying a drift correction considerably improves the Signal-to-Noise ratios.

In conclusion, although our results augur much better for the FPS/Detector system performances than it has been reported up to now, it is clear that more work is still needed in order to reduce the amount of data that have to be discarded.